Finite element modeling of multiple electrode submerged arc welding of large diameter pipes

Finite element modeling of multiple electrode submerged arc welding of large diameter pipes

A Khudyakov [1], Yu Korobov [1,4], P Danilkin[2,3] and V Kvashnin[2,3]

[1] Ural Federal University named after the first President of Russia B.N. Yeltsin, Yekaterinburg, Russian Federation
[2] The Russian Research Institute of the Tube & Pipe Industries, Chelyabinsk, Russian Federation
[3] South-Ural State University (National Research University), Chelyabinsk, Russian Federation
[4] M.N. Mikheev Institute of Metal Physics of the Ural Branch of the Russian Academy of Sciences, Yekaterinburg, Russian Federation

E-mail: Aohudyakov@gmail.com; Yukorobov@gmail.com; DanilkinPA@gmail.com.

Abstract. For the process of multiple-electrode submerged arc welding (MESAW) of large-diameter pipes (LDP) a mathematical model has been developed with a numerical solution in the software product "SYSWELD". The paper defines the parameters of double ellipsoid model of heat sources by J. Goldak. Using regression analysis of experimental data empirical formulas for calculating geometrical parameters of heat sources model by J. Goldak and deposition rate were developed for welding with direct current on positive polarity and alternating current. The model allows to predict the shape of weld and to estimate analytically the cooling rate in the heat affected zone (HAZ). The developed model and its numerical solutions with sufficient accuracy for practical calculations reflect the process of longitudinal welding of LDP.

1. Introduction

Modern production of large diameter pipes implies welding of a longitudinal weld in two passes by means of MESAW after assembling by gas metal arc welding. Welding is accompanied by a large number of physicochemical processes associated with heating, melting, cooling, crystallization of the weld metal and structural transformations of the base metal in the HAZ. Thermal impact has the decisive influence on the nature and kinetics of thermomechanical and physical processes of arc welding, and subsequently on the microstructure and mechanical properties of welded joints [1, 2, 3]. According this there is no doubt the relevance of the calculation of temperature fields during MESAW of high-strength LDP for their further use in solving problems related to structure formation, mechanical properties of welded joints and dimensions of the weld and HAZ.

2. Finite element modelling

During MESAW heat input into the product is simultaneously carried out by several volumetric sources, therefore the temperature fields in the studied plane are determined according to the principle of superposition by the sum of temperature fields from each heat source (figure 1):

$$T_a(q_\Sigma, r, t) = \sum_{n=1}^{i} T_i(q_i, r, t), \quad (1)$$

Where Ta – field of temperatures on the studied plane; q_Σ – total heat input of welding; q_i – heat input of i-th heat source; r – radius vector; t – time.

For modelling of volumetric density of heat generation in the vicinity of each welding arc, the model of volumetric heat generation proposed by J. Goldak [4, 5, 6] was used. The model of the heat source by J. Goldak is described by the normal distribution of the specific thermal power over all coordinate axes in the volume of the body having the form of a double ellipsoid (Figure 2).

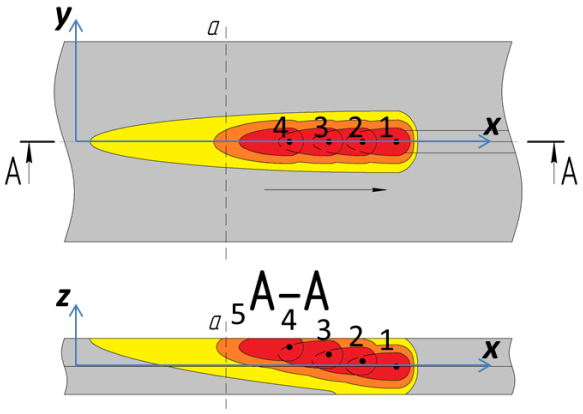

Figure 1. Scheme of thermal fields during MESAW

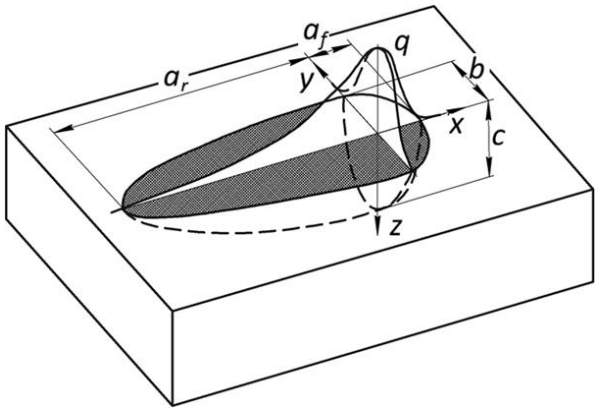

Figure 2. Model of double ellipsoidal heat source by J. Goldak

The independent distribution of the specific heat power qv in the frontal (index f) and tail (index r) parts of the ellipsoid is described by the equations [7, 8]:

$$q_{v,f} = f_f \cdot \frac{6\cdot\sqrt{3}\cdot q}{a_f \cdot b \cdot c \cdot \pi^{3/2}} \cdot \exp\left(-3\cdot\left(\left[\frac{x+v\cdot(t-\tau)}{a_f}\right]^2 + \left[\frac{y}{b}\right]^2 + \left[\frac{z}{c}\right]^2\right)\right), \quad (2)$$

$$q_{v,r} = f_r \cdot \frac{6\cdot\sqrt{3}\cdot q}{a_r \cdot b \cdot c \cdot \pi^{3/2}} \cdot \exp\left(-3\cdot\left(\left[\frac{x+v\cdot(t-\tau)}{a_r}\right]^2 + \left[\frac{y}{b}\right]^2 + \left[\frac{z}{c}\right]^2\right)\right), \quad (3)$$

where q – the effective thermal power of the heating source; τ – the delay time, counted from the beginning of the source action; t – the current time; v – source movement speed (welding speed); x, y, z – semiaxes of the ellipsoid in the direction of the coordinate axes OX, OY, OZ; ff and fr – the coefficients that determine the ratio of heat introduced into the frontal and tail parts of the ellipsoid; af, ar, b, c - the corresponding radiuses of the normal distribution.

According to the theory of heat propagation in a solid [9] a scheme of a fast moving point heat source in a flat layer was taken. The heat power distribution was represented by Goldak's model of a double ellipsoid. Common dependencies of the specific heat, thermal conductivity and total surface heat transfer [10, 11] on body temperature for low carbon steel were used in the developed finite element model. The introduction of heat into the edges during MESAW was represented as separate volumetric heat sources from each arc. Figure 3 shows adopted scheme of the temperature boundary problem.

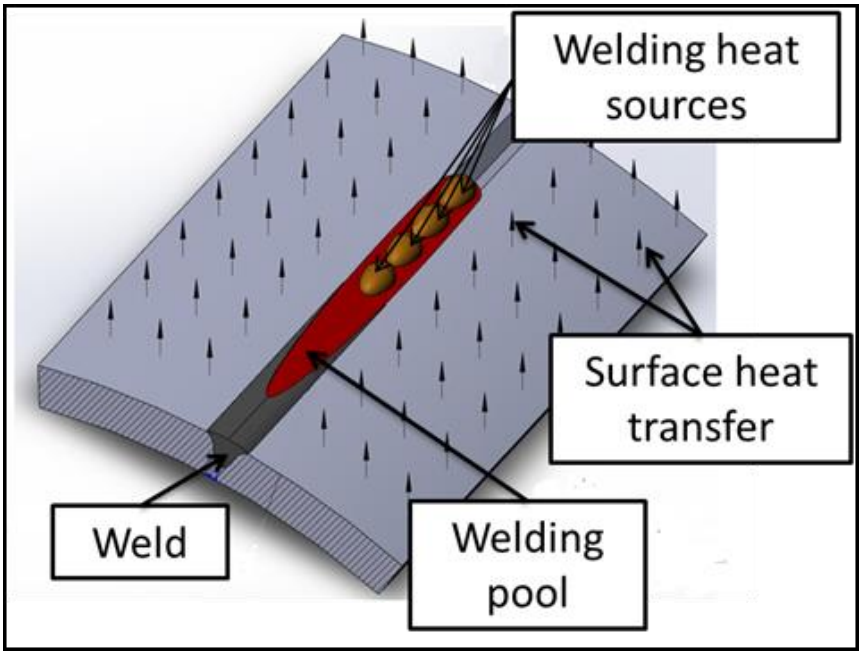

Figure 3. Temperature boundary problem for MESAW of LDP.

Welding of a longitudinal seam of a LDP is carried out in a special edge bevelling. Since each welding arc deposits a certain amount of molten metal, each welding heat source acts on a different depth. The first heat source acts in the root of the edge bevelling, the second source acts on the surface of the weld metal deposited by the first arc, the third - on the surface of the weld metal deposited by the second arc and etc. The scheme of heat sources distribution in depth is presented in Figure 4.

The Z coordinate of each subsequent heat source will be determined as the height of the triangle with an area equal to the cross-sectional area of the metal deposited by the previous welding arcs. The scheme for determining the Z coordinate of heat sources during MESAW is shown in Figure 5.

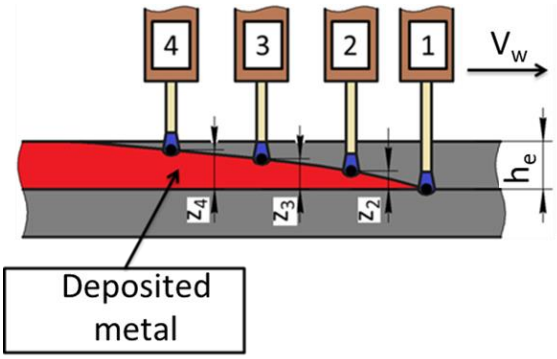

Figure 4. The scheme of heat sources distribution in height: h_e - the depth of edge bevelling; Z_i - coordinates of the i-th heat source.

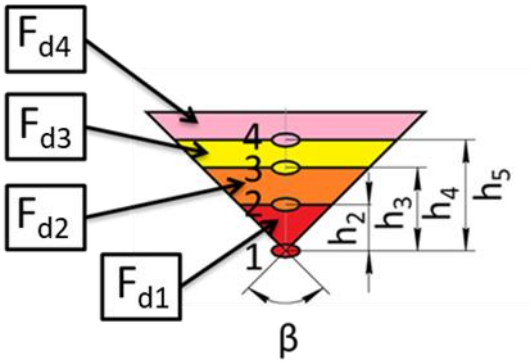

Figure 5. The scheme for determining the Z coordinate of heat sources: F_{di} – the cross-sectional area of the deposited metal by the i-th arc; β – angle of edge bevelling.

The Z coordinate of each heat source was determined from the expression of the height of a triangle by a known area using the equation:

$$Z_i = \sqrt{\frac{\sum_{i=1}^{n}(F_{d_{i-1}})}{\tan(\beta/2)}}, \quad (4)$$

where F_{di} – the cross-sectional area of the deposited metal.

The cross-sectional area of the metal Fn deposited into the welding pool by each arc is determined by the equation:

$$F_d = \frac{\alpha_m \cdot I_w}{\gamma \cdot V_w}, \quad (5)$$

where α_d – the deposition coefficient, for submerged arc welding is equal to the melting coefficient α_m; I_w - welding current; γ - the density of the deposited metal; V_w - welding speed.

To calculate the cross-sectional area of the deposited metal empirical dependences of melting coefficients were obtained for welding with direct current of positive polarity ($\alpha_{d(DC+)}$) and alternating current ($\alpha_{d(AC)}$) for electrode ejection of 40 mm. Dependences were obtained using the method of regression analysis of experimental data.

$$\alpha_{d(DC+)} = 0{,}053 \cdot \frac{I_w}{d_e^{0{,}88}}; \quad (6) \qquad \alpha_{d(AC)} = 1{,}257 \cdot \frac{I_w^{0{,}539}}{d_e^{0{,}514}}, \quad (7)$$

where I_w – welding current; d_e – electrode diameter.

Basing the developed model, simulation of the cooling rates in CGHAZ was carried out using SYSWELD software package (license agreement No 2910-2014 ДУ). In the Sysweld software the power distribution of volumetric heat sources is carried out according to the algorithm in accordance with equations (2, 3). The heat of the electric arc enters the edges through the surface of forming crater, i.e. through the volumetric heat source. That is why in the developed finite element model it was assumed that the geometrical parameters of the heat sources by Goldak are equal to geometrical parameters of the crater of the weld pool that forms under a welding arc. Therefore, to determine the parameters of the crater depending on welding modes parameters additional studies were conducted. To determine the parameters of the crater a technique based on the use of inserted tungsten indicators [12, 13] was used. For this tungsten wires were inserted into the plate subjected to welding in the plane perpendicular to the welding direction (figure 6). Wires with a diameter of 0.5 mm and with a step of 1.5 - 2 mm were used.

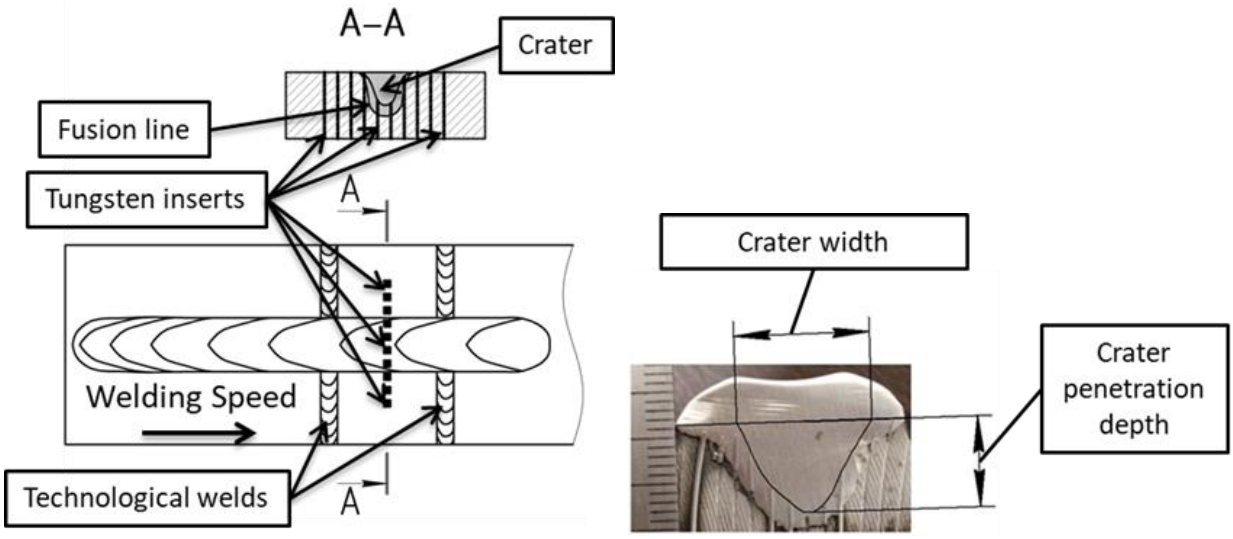

Figure 6. Determination of geometrical crater parameters: a) Scheme of plate with tungsten inserts; b) Crater geometrical parameters.

The results of the experimental data were processed using regression analysis, as a result of which empirical dependences of the geometric parameters of the crater from the parameters of welding modes were obtained:

$$h_{cr}^{DC+} = 2{,}123 \cdot \frac{I_w^{1,516}}{V_w^{0,528} \cdot d_e^{0,488}} \quad (8); \qquad b_{cr}^{DC+} = 54{,}205 \cdot \frac{U^{1,216} \cdot d_e^{0.904}}{I_w^{0,829} \cdot V_w^{0,571}} \quad (9);$$

$$h_{cr}^{AC} = 0{,}642 \cdot \frac{I_w^{1,168}}{U^{0,756} \cdot V_w^{0,756} \cdot d_e^{0,923}} \quad (10); \qquad b_{cr}^{AC} = 6{,}865 \cdot \frac{U^{0,851} \cdot d_e^{0.6}}{I_w^{0,851} \cdot V_w^{0,32}} \quad (11),$$

where h_{cr}^{DC+}, h_{cr}^{AC} – crater depth during welding with a direct current on positive polarity and alternating current, respectively; b_{cr}^{DC+}, b_{cr}^{AC} – crater width during welding with a direct current on positive polarity and alternating current, respectively; U - voltage.

The modeling of the welding process was performed in accordance with the industrial standard welding modes of LDP. Graphic images of the numerical solution of the finite element model are presented in Figure 7. The developed finite element model with sufficient accuracy for practical purposes provides prediction of the geometric parameters of the weld (Figure 8) and the cooling rate (Figure 9) in coarse grained heat affected zone. The error does not exceed 10%.

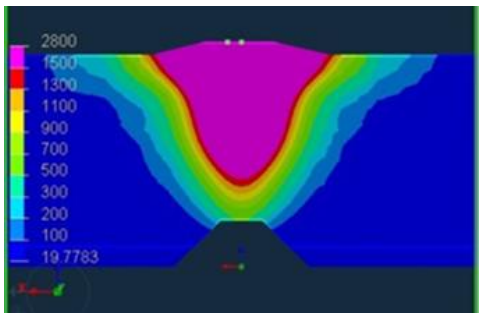

Figure 7. Model of multiple-electrode SAW weld shape applying to the 1153x30.9 mm pipe, inner weld.

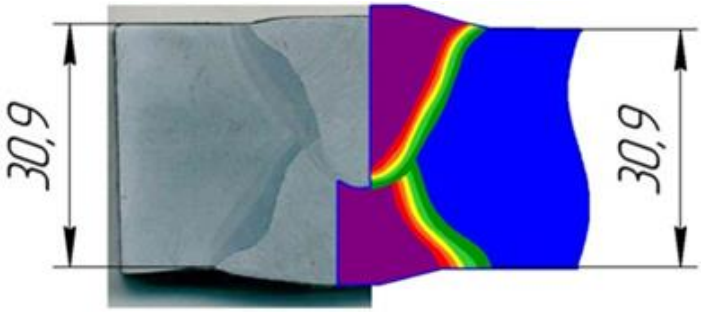

Figure 8. Comparison of the geometric parameters of the real weld and its model applying to the 1153x30.9 mm pipe.

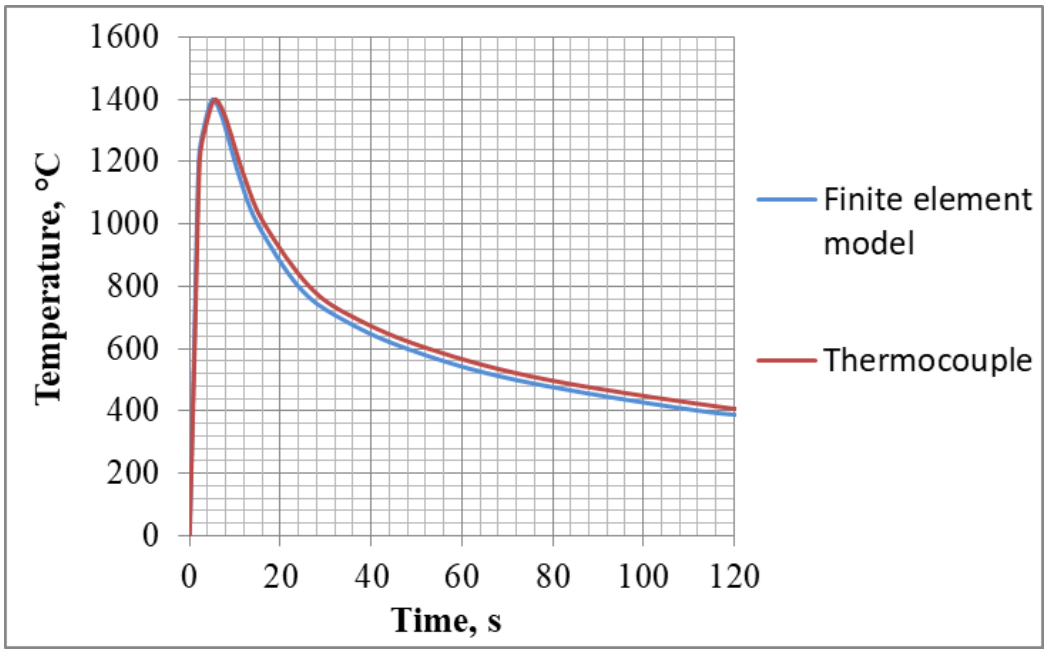

Figure 9. Thermal cycle of welding in coarse grained heat affected zone.

3. Conclusions

The parameters of heat sources by J. Goldak were determined for the finite element modeling of the heat distribution process during multiple electrode submerged arc welding of large-diameter pipes. Also using regression analysis of experimental data empirical equations have been developed for calculating melting coefficients for welding with direct current on positive polarity and alternating current.

A mathematical model of multiple electrode submerged arc welding with a numerical solution in the SYSWELD software was developed. The model allows to predict the shape of weld and to estimate analytically the cooling rate in the heat affected zone (HAZ). The developed model and its numerical solutions with sufficient accuracy for practical calculations reflect the process of longitudinal welding of LDP.

Acknowledgments

This work was done within the state order of IMP UB RAS on the subject “Laser”.

References

[1] B.M. Berezovsky, 2006, Mathematical models of arc welding, Vol. No1, Chelyabinsk, 547 p. (in Russian).
[2] B.M. Berezovsky, 2006, Mathematical models of arc welding, Vol. No5, Chelyabinsk, 645 p. (in Russian).
[3] V.A. Karhin, 2013, Thermal processes during welding. St. Petersburg, 646 p. (in Russian). Goldak J., Chakravarti A., Bibby M. A new finite element model for welding heat source // Metallurgical Trans. B. — 1984. — 15B. — pp. 299-305.
[4] Goldak J. Akhlaghi M. Computation welding mechanics, Springer Science + Business Media Inc., Boston, 2005.
[5] Goldak J. Computer modelling of heat flow in welds / J. Goldak, M. Bibby, J.Moore, R. House, B. Patel // Metallurgical Transactions, 1986. V.17B. P. 587-600.
[6] Koch F. Simulation of the temperature field and the microstructure evaluation during multi-pass welding of L485MB pipeline steel / F. Koch, M. Enderlein, M. Pietrzyk // Computer methods in material Science. Vol. 13, No1, 2013, pp. 173-180
[7] O.A. Slyvinskyy, A. O. Prepiialo, V.L. Bondarenko, V. P. Slyuta, 2014, “Calculation and experimental analysis of thermal processes of thin-sheet stainless steel welding using TIG and CMT methods”, Technological Systems, No 1, 2014, pp. 76-82.
[8] N.N. Rykalin, 1951, Calculations of thermal processes during welding. Moscow, 296 p. (in Russian).
[9] Konovalov, A. Kurkin, E. Makarov, V. Nerovnij and B. Yakushin, 2007, “Theory of welding processes” Moscow, 752 p. (in Russian).
[10] K. Bagryanskij, Z. Dobrotina, K. Hrenov, 1976, “Theory of welding processes”, Kiev, 424 p. (in Russian).
[11] A.V. Savinov, 2013, “Improving the technological properties of the arc at TIG welding”, Phd diss. Volgograd, Russia. 243 p. (in Russian).
[12] V.I. Atamanuk, 2008, “Development of ways and means to improve the stability of welds formation during welding with non-consumable electrode” Phd diss. Volgograd, Russia. 153 p. (in Russian).